

AE monitoring of a two-span model masonry arch bridge subjected to pier scour

S. Invernizzi, G. Lacidogna, A. Manuello & A. Carpinteri
Politecnico di Torino, Torino, Italy

ABSTRACT: A scaled model of a two-span masonry arch bridge has been built in order to investigate the effect of the central pile settlement due to riverbank erosion. The bridge geometry and the structural details, including the masonry bricks and mortar joints, are realized in the scale 1:2. The model bridge has been equipped with different Non Destructive Testing (NDT) instruments, including accelerometers, displacement transducers LVDT, strain gages, optic fibres strain sensors, and Acoustic Emissions (AE). Although this technique has been already attempted in the past, a relation between the AE count and location, and the structural integrity has only recently been proposed by the authors, and it is useful to verify its applicability in the case of imposed differential settlement induced by the pier scour. The model bridge has been subjected to incremental settlement of the pile, which was sustained on a mobile support. The exact mechanism and temporal evolution of the pier scour has been investigated numerically and experimentally by mean of an hydraulic model. In the present paper a detailed description of AE data and damage localization is provided. During the first stage of the settlement, the AE counting has been recorded. Based on the interpretation of the AE rate, it is possible to monitor the criticality of the ongoing process. In addition, thanks to an equipment with six AE piezoelectric transducers, it is possible not only to detect the ultrasonic emissions, which are due to the propagation of cracks, but also to locate the main damage zones. The evolution of damage has been also interpreted numerically with the aid of a finite element program able to predict the nucleation and propagation of fracture. In this way, some criteria for the monitoring and interpretation of full-scale structure cracking are provided for the assessment in presence of riverbank erosion phenomena.

1 INTRODUCTION

Masonry arch bridges are extremely stiff structures, which are well suited to sustain high gravity loads but are very vulnerable with respect to differential settlements of the supports. In the case of multi-span arch bridges traversing rivers, the phenomenon preferably takes place in occasion of the flood peaks. The pier scour is one of the worst dangers for the integrity of historical bridges.

It is worth noting that the problem has a very important social impact, especially in countries like Italy that have a wide historical heritage. Consider that, even limiting the case to the northern region Piedmont, the masonry bridges are a few hundreds. In recent years, different approaches have been attempted for monitoring the evolution of the phenomenon and to provide the necessary warning in the case of structural collapse. The main weak points of such techniques are that they cannot be used during the flood peaks and that they provide poor information about the overall integrity of the bridge.

In this context, structural monitoring (Carpinteri & Bocca, 1991) can be an effective complement to hydro-geological monitoring, since it could provide information about the propagation of damage and on the necessity of a quick intervention. The NDT combined approach, with the use of dynamic analysis, optic fibre sensors, and AE acquisitions, provides a slightly invasive procedure, which is particularly targeted to historical cultural heritage. On the other hand, performing different types of acquisitions and analyses is the only way to increase the robustness of the integrity assessment.

Among the different NDT's, the AE will be considered with more details in the following (Othsu, 1996), in combination with the numerical model of cracking. Although this technique has been already attempted in the past (Royles & Hendry, 1991), a relation between the AE count and the structural integrity has only recently been proposed (Carpinteri & Lacidogna, 2001, Carpinteri et al. 2007), and it is useful to verify its applicability in the case of imposed differential settlement induced by the pier scour.

2 THE BRIDGE MODEL

The model bridge has not been obtained from a real bridge geometry, but has been designed according to historical rules for the geometry definition and shares most of the characteristics of real historical bridges. Then, according to the theory of models, the geometry has been scaled down to obtain the model dimensions. The scale of the model bridge is 1:2. The model bridge is 5.90 m long and 1.60 m depth. Each masonry brick is hand made, and has a size of 130x65x30 mm, according to the geometrical scale proportion. Strength and stiffness of masonry brick and mortar have been selected to be rather limited, to better reproduce the case of real historical bridges.



Figure 1. Model bridge realized at the Politecnico di Torino laboratories.

The two masonry arches of the model bridge (Figure 1) are supported by two masonry abutments and a central pier built with the same masonry. The abutments lay on concrete basements that are linked to the ground through special reinforcements.

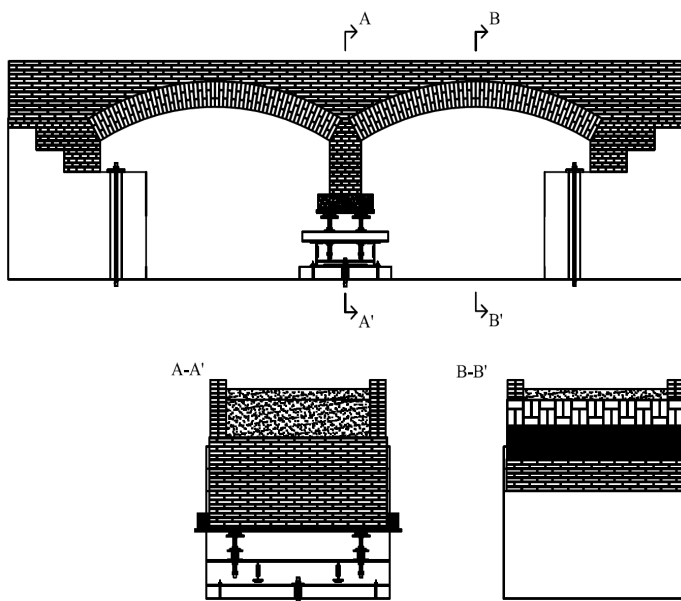


Figure 2. Lateral view and sections in correspondence of the central pier and of the mid-span.

Above the arches, there are containment masonry walls on the four sides of the bridge, which provide

the location for the filling material. The upper part of the bridge is completed with a concrete slab top, realized with limited cement content. In the central part of the bridge, above the pier, a load will be concentrated to simulate the weight of the pier foundation, which was not explicitly realized in the model.

A scheme of the model bridge is showed in Figure 2, together with the mobile steel support of the central pier that, thanks to four screws, allows for the imposition of the differential settlement. Note that the base of the pier does not lay directly on the steel plate, but on a high density polystyrene cushion, which will be removed partially during the test in order to simulate in the details the effect of confinement lost during the erosion process.

The density of this polystyrene support has been designed to properly correspond to the foundation soil characteristics. The exact mechanism and temporal evolution of the pier scour has been investigated numerically and experimentally (Figure 3) in collaboration with the Department of Hydraulics and Transportations of the Politecnico di Torino.

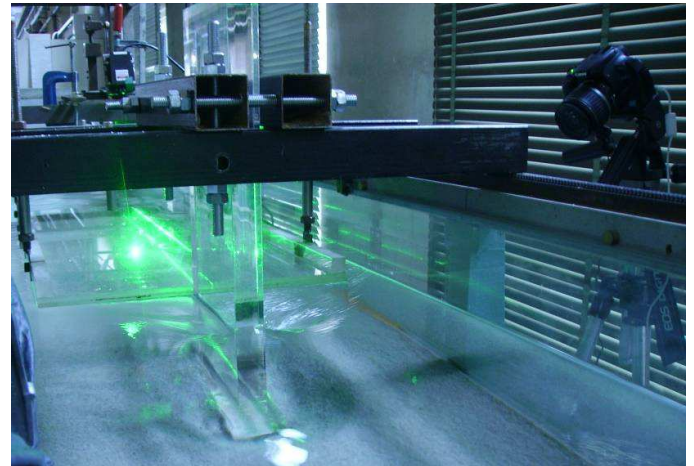


Figure 3. Experimental study of the pier scour evolution.

During the test, digital camera and laser scanner acquisitions have been performed. The analysis of the results suggests that a good approximation of the phenomenon is obtained providing to the model bridge pier a linear differential settlement transversal to the bridge longitudinal axis.

Prior to the application of the differential settlement, it is useful to have an estimate of the model bridge mechanical response. Two aspects are of main concern: how the dynamic behaviour of the bridge will be affected, and where the deformation and damage will localize. In fact, gaining those information allows for a better positioning of the measurement instruments and an optimized tuning of the acquisition resolution.

The first mechanical parameters to collect are those of the base material, i.e. the masonry. Therefore, a number of laboratory tests have been performed (Figure 4), including compression tests, di-

agonal compression tests, three point bending tests on masonry arches, and shear tests. In addition, tests on the mortar alone, and on the concrete used to support the abutments have been performed. The main mechanical parameters obtained are: the Young's modulus E , the Poisson ratio ν , the tensile strength f_t , the compressive strength f_c , and the tensile fracture energy G_F . These parameters are the few necessary for the numerical simulation described in the following section.

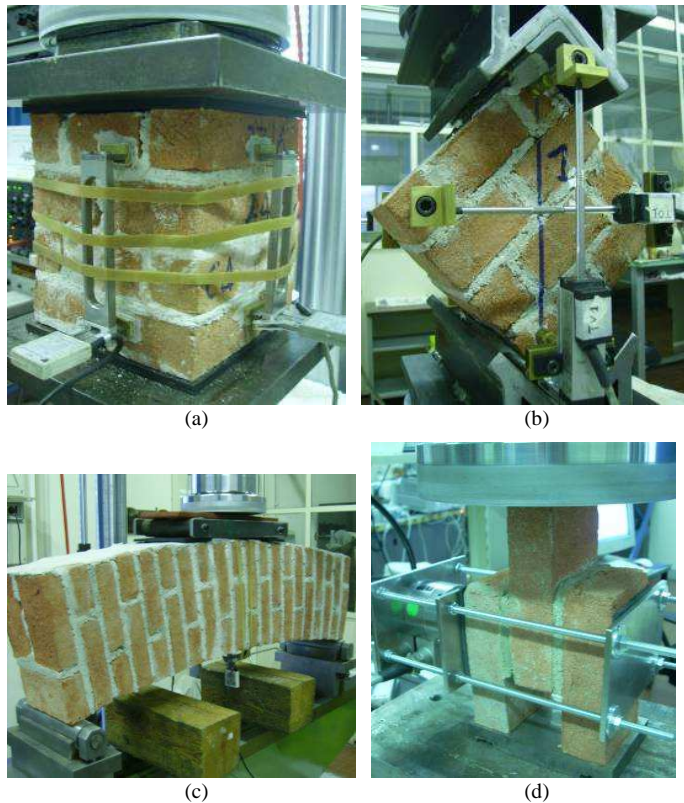


Figure 4. Laboratory tests for the mechanical characterization of the masonry: compression test (a); diagonal compression test (b); three point bending of a masonry arch (c); shear test (d).

3 NUMERICAL PREDICTION OF DAMAGE

The numerical prediction of damage has been performed developing a nonlinear finite element model of the bridge with the help of the commercial code iDIANA (Manie, 2009). The geometry of the model accounts for all the main parts of the bridge: the masonry arches and the pier, the masonry abutment and the underlying concrete foundation, the masonry containment walls above the arches, the filling material, and, above all, the poor quality concrete slab. In addition, the polystyrene cushion below the masonry pier has been explicitly modelled, as well as the interface in correspondence of the movable support under the pier and the additional load on top of the bridge. In a first instance, the geometrical nonlinearity has been disregarded. On the other hand, all the potential sources of mechanical nonlinearity have been considered. In order to assess the damage localization in the model, a smeared crack approach was

followed, both for masonry and concrete. In both cases, the adopted constitutive law is characterized by a limit compression strength and a limit tensile strength with linear softening. The simplicity of such hypothesis is preferred with respect to much more complicated material models, since very few mechanical parameters are required. The filling material, on the other hand, has been considered a very poor (i.e. with very limited stiffness) elastic material. The interface at the pier footing has a no-tension constitutive law, which allows for an explicit evaluation of the actual contact area. The mechanical parameters of the different components are shown in Table 1. The model mesh has been built with three-dimensional quadratic brick elements for the continuum part, and with special quadratic interface elements for the central support. The whole model is composed of approximately 18000 elements connected by approximately 82000 nodes.

Table 1. Mechanical material parameters adopted in the nonlinear analysis.

	γ [kg/m ³]	E [Pa]	ν	f_c [Pa]	f_t [Pa]	G_F [Nm]
Concrete	2400	$3 \cdot 10^{10}$	0.15	---	---	---
Masonry	1900	$1.5 \cdot 10^9$	0.2	$3 \cdot 10^5$	$4.3 \cdot 10^6$	400
Slab Concrete	2200	$5 \cdot 10^9$	0.15	$3 \cdot 10^5$	$4.3 \cdot 10^6$	100
Filling	2000	$5 \cdot 10^7$	0.49	---	---	---
Polystyrene	40	$1.01 \cdot 10^7$	0.2	$2.8 \cdot 10^5$	$4.3 \cdot 10^6$	10

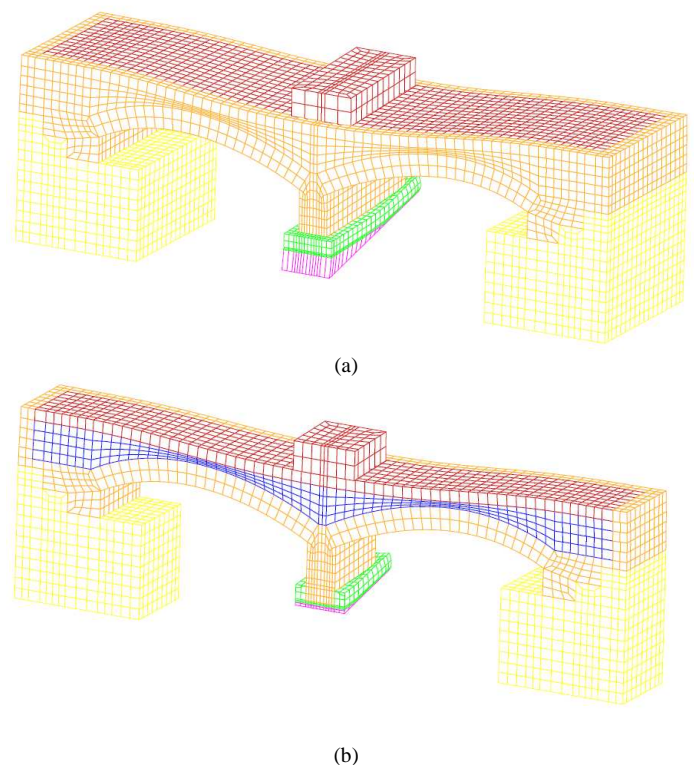


Figure 5. deformed mesh of the complete model (a), longitudinal section of the model, showing the internal structure (b).

The load is applied in two main sequences. First, the dead load is applied together with a small uniform uplift of the central pier support. This displacement

is imposed to better account for the building construction procedure, and avoids the formation of spurious traction in the model, before the differential settlement is applied. In a second phase, the differential settlement with an upper bound of 20 mm is applied incrementally to the central pier. An automatic step bisection algorithm is used to improve the convergence.

The deformed mesh of the model is shown in Figure 5, where the various materials have different colors. Figure 5b is a longitudinal section of the model that shows the internal structure of the bridge.

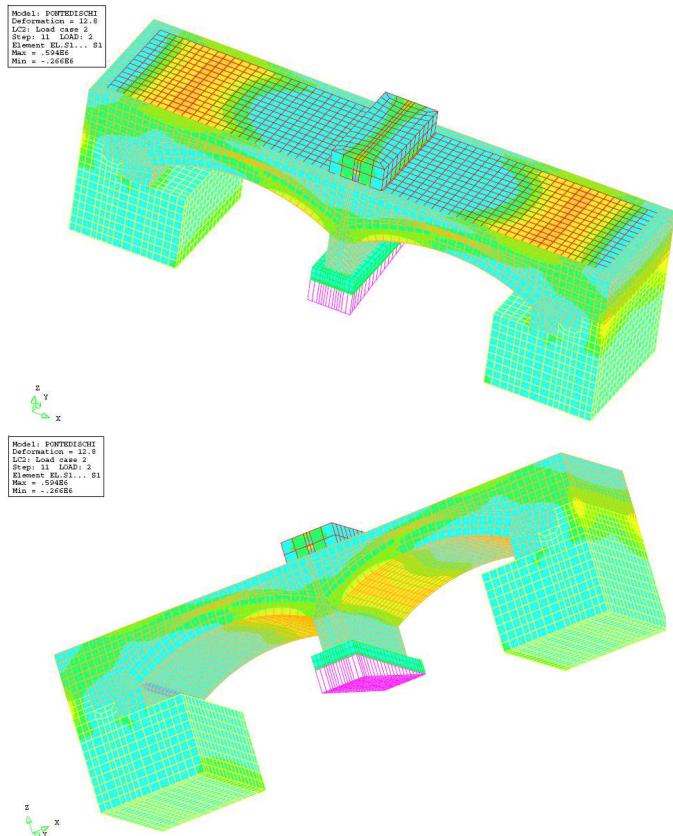


Figure 6. Tensile principal stress contours.

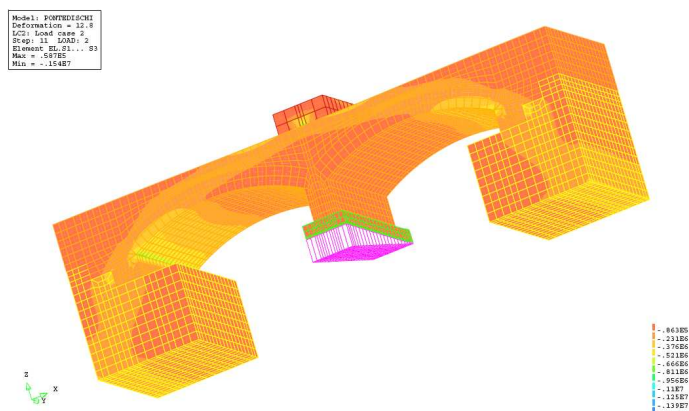


Figure 7. Compressive principal stress contour.

The contours of the principal tensile stresses (Figure 6) show that the highest tractions are localized in the arches intrados close to the central pier, as well as in the extrados of the bridge (i.e. in the

poor quality concrete slab) closer to the abutments. In those regions the sensors will be localized to measure the strain (strain gages, optical strain sensors). On the other hand, LVDT sensors will be put to monitor the pier support, in order to detect the decompression of the pier.

Figure 7 shows the contour of the minimum principal stress. It is straightforward to notice that an arch mechanism is activated between the two external abutments, which tend to hide the effect of the simulated pier scour. This phenomenon is very important and dangerous, since the overall behavior of the bridge is made more brittle.

Thanks to the nonlinear analysis, it is also possible to assess where cracks will enucleate and propagate in the model. This result is shown in Figure 8. Three main zones are detected: in the masonry arches intrados, at about 0.4m away from the central pier abutment; at the interface between the containment masonry wall and the concrete slab, approximately at the mid-span of the arches; and in the concrete slab extrados right above the external abutments. This information will help the positioning of LVDT sensors to measure the crack aperture and will be compared with the localization of the AE sources.

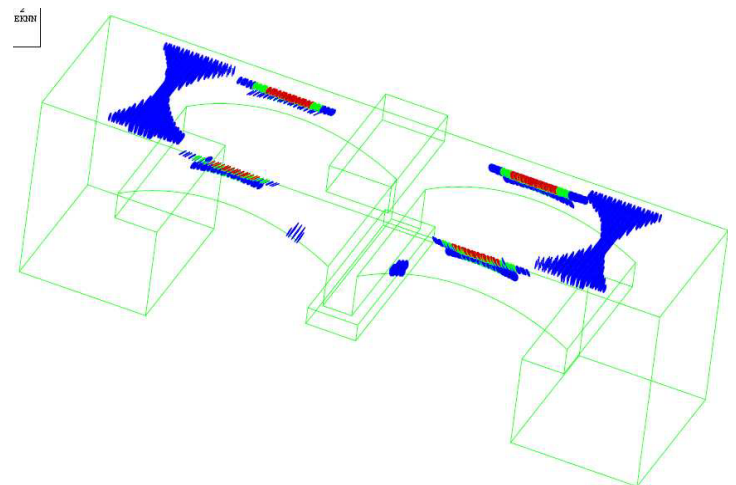
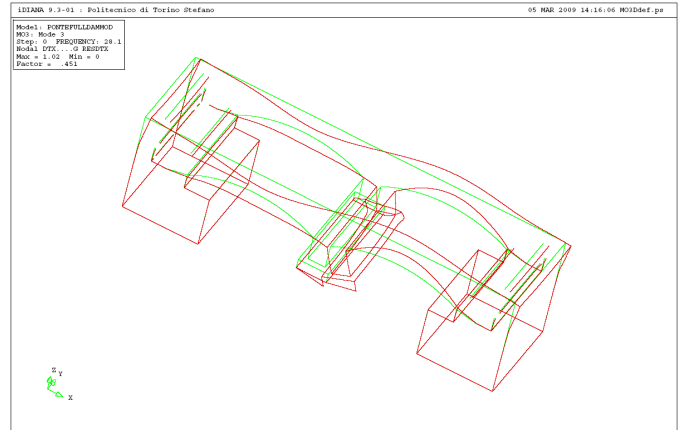
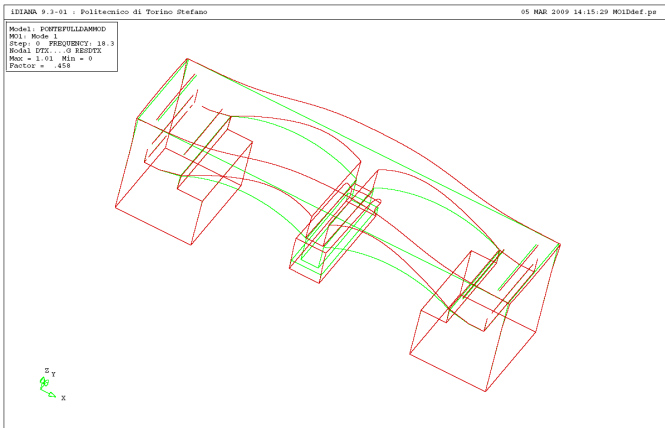
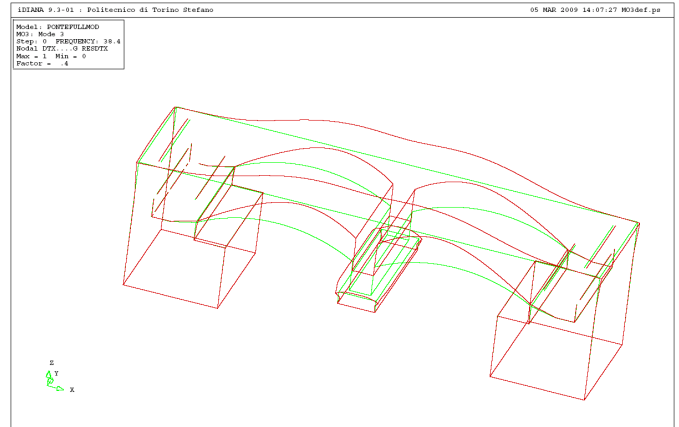
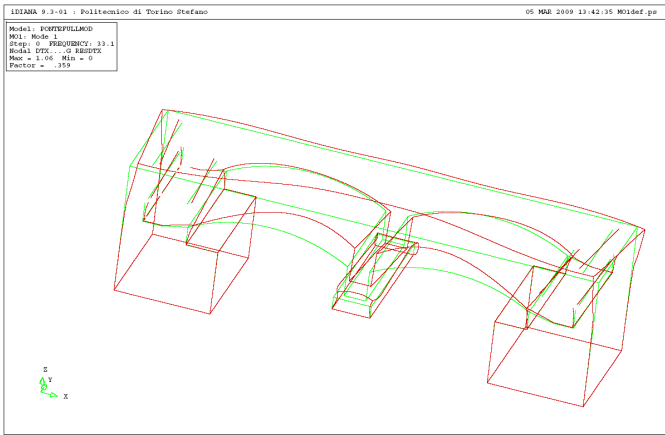


Figure 8. Smearred crack pattern corresponding to the maximum differential settlement (2 mm).

Table 2. Shift of the Eigen-frequencies due to damage propagation.

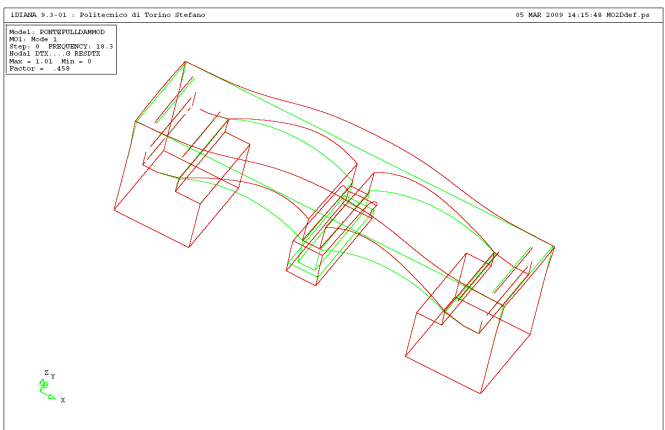
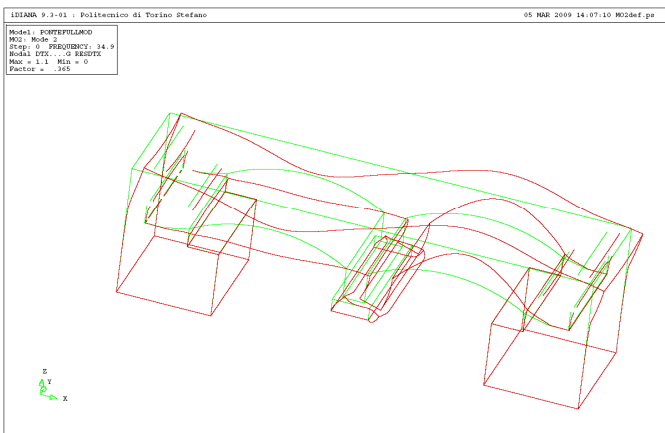
Eigen-mode	Eigen-frequency [Hz]	
	Undamaged	Damaged
First	27.1	15.3
Second	32.4	25.0
Third	35.9	25.3

In order to provide some hints for the dynamic identification of the model, two modal analyses have also been performed. The first analysis has been carried out prior to the damage propagation. The Eigen-frequencies, shown in Table 2 and Figure 9 (left column), compare well with a preliminary experimental identification of the model.



(a)

(c)



(b)

Figure 9. Modal shapes before (above) and after (below) damage propagation: first mode (a); second mode (b); third mode (c).

A second analysis has been performed with the secant stiffness matrix, after the differential displacement application. This kind of analysis is basically linear, and cannot account directly for the unilateral behaviour of cracks. Nevertheless, it provides us an estimate of the foreseen Eigen-frequencies shift due to damage, and then will help us in better tuning the dynamic acquisition resolution. The effect of damage is expected to be sensible, as emphasized by the comparative results in Table 2. Note also that the modal shape of some of the first natural modes is also expected to change qualitatively (Figure 9).

4 AE MONITORING

The cracking process taking place in some portions of the masonry vault during the loading test was monitored using the AE technique. Crack advancement, in fact, is accompanied by the emission of elastic waves, which propagate within the bulk of the material. These waves can be captured and recorded by transducers applied to the surface of the structural elements.

The AE measurement system used by the authors consists of six piezoelectric (PZT) transducers, calibrated on inclusive frequencies between 50 and 500 kHz, and six control units. The AE sensors were placed at the intrados of one of the bridge vault, in order to cover six almost equal competence areas

(Fig. 10). Thanks to the symmetry of the structure and of the loading scheme, it was possible to put limit to the AE acquisition to one only of the two vaults. This allowed for an optimized coverage with the available sensors.

The oscillation counting limit was fixed at 255 oscillations every 120 seconds (Carpinteri & Laciogna, 2001, Carpinteri et al., 2006). This procedure is referred to as Ring-Down Counting, where the number of counts is proportional to crack advancement. The number of counts (N) is obtained by determining the number of times that the signal crosses a certain threshold voltage. The crack growth rate is related to the voltage amplitude of the AE elastic wave.

The attenuation problem can be overcome by reducing to a few meters the distance of the transducers from the signal generation point. In this way, it can be assumed that the system of measurement is able to detect the most meaningful AE events reflecting the evolution of cracking phenomena in the bridge. Utilizing the Ring-Down Counting method, and neglecting the material attenuation properties, the AE counting number (N) can be assumed proportional to the quantity of energy released in the masonry volumes during the loading process.

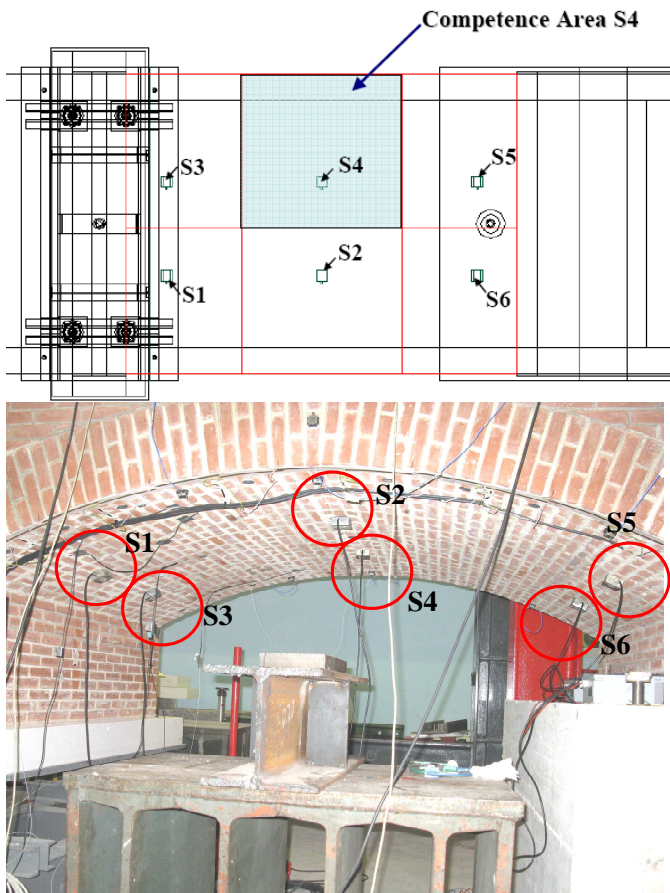


Figure 10. Positioning of the acoustic emission transducers, and their competence area.

The recorded AE events are shown in Figure 11 as a function of time and compared to the stepwise application of the differential settlement. The cumu-

late AE curves emphasize the different amount of events in the different competence areas. This result is also displayed with the aim of shaded grey diagrams in Figure 12.

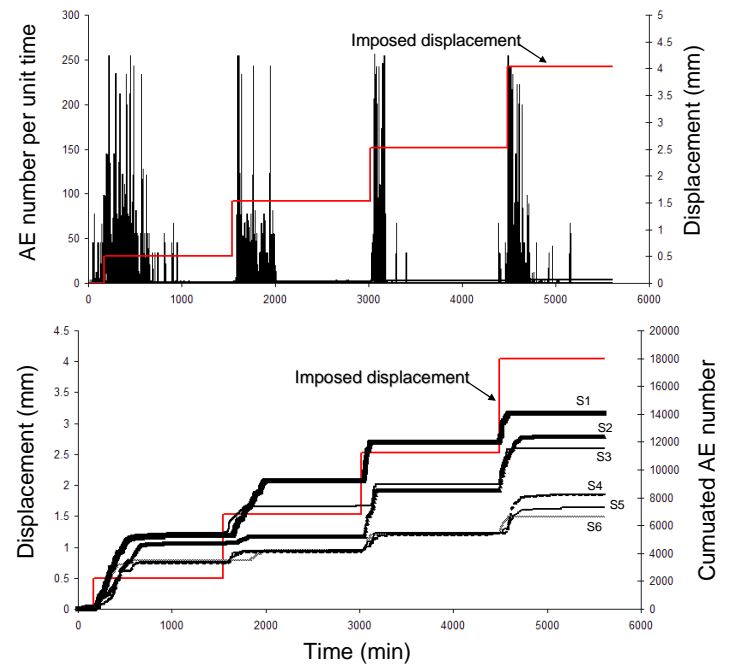


Figure 11. AE rate and cumulative AE as a function of time, compared with the progression of the imposed settlement.

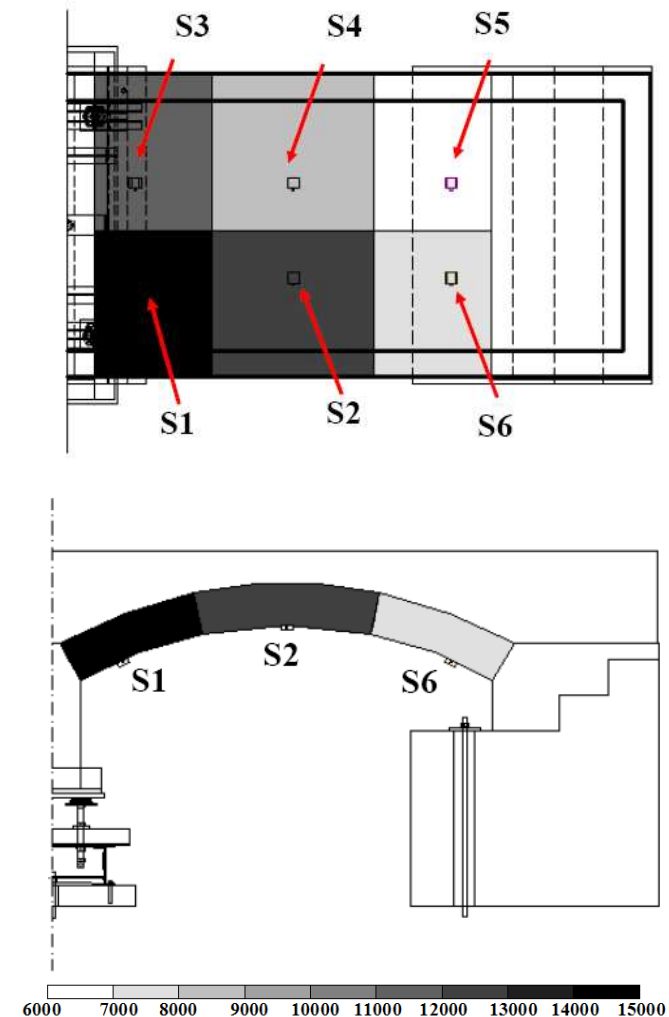


Figure 12. Number of acoustic events in each competence area.

The regions with the larger amount of emissions correspond correctly to the most fractured areas detected visually.

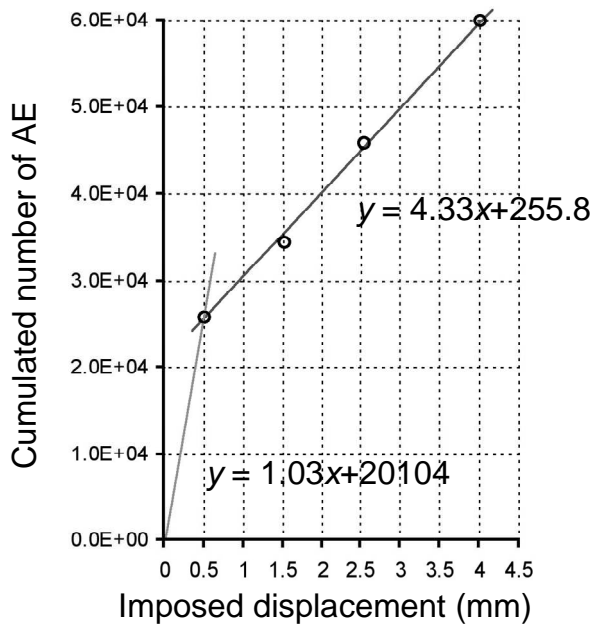


Figure 13. Evolution of the acoustic emission rate.

Figure 13 shows the evolution of the AE rate as a function of the imposed displacement. The first stage presents a steeper slope, due to the extremely brittle nature of the fracture nucleation.

On the other hand, the AE rate converge to a lower level as the settlement increases. This reveals a quite stable crack propagation process. It is expected that the AE rate will increase again when the system, due to the evolution of the imposed displacement, will reach a critical stage.

4.1 Numerical simulation of fracture

The experimental crack pattern was acquired by a careful visual inspection as well as by means of LVDT and optical fibre sensors.

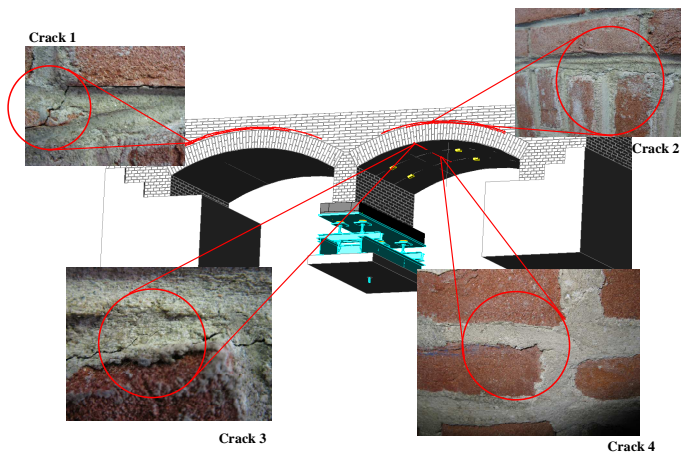


Figure 14. Comparison between the experimental and numerical crack pattern.

Figure 14 shows that the experimental crack pattern, characterized by transversal cracking at the intrados of the vaults close to the central pier, and lateral cracking in correspondence of the arches extrados, were correctly simulated by the numerical model (Figure 8).

On the other hand, the transversal cracking obtained numerically in the concrete slab above the filling, was not detected experimentally. In place of that, a detachment between the concrete slab and the masonry wall at the end of the bridge was visible (Figure 15). In order to be able to model this phenomenon, it is necessary to model explicitly the interface between the two materials.

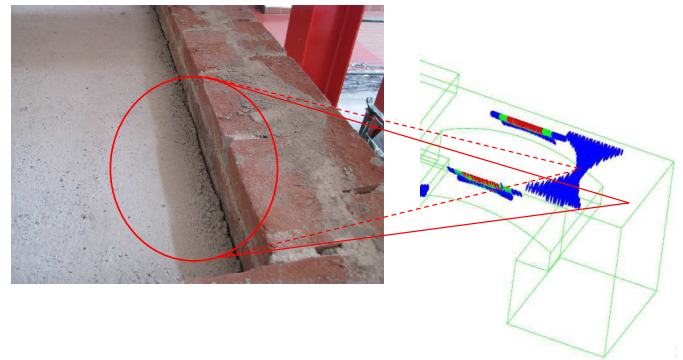


Figure 15. Detail of the detachment between the concrete slab and the masonry wall at the end of the bridge compared with the numerical previsions.

5 CONCLUSIONS

A laboratory scaled model masonry bridge has been built for the experimental analysis of the pier scour phenomenon. The amount and shape of the differential settlement due to the pier scour was experimentally evaluated by means of hydraulic tests. During the application of the differential settlement, the bridge has been monitored with several non-destructive techniques, including Acoustic Emission, optical fibers, and dynamic identification.

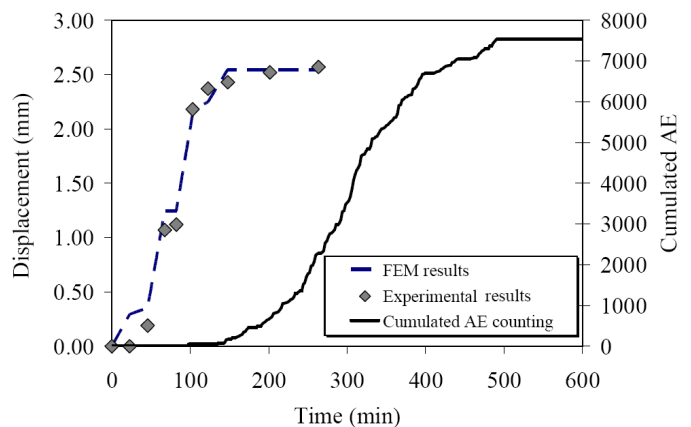


Figure 16. Comparison between cumulated AE counting (right y-axis), and the experimental or numerical vertical displacements (left y-axis) (Carpinteri et al. 2007).

The numerical study of the test has been presented.

Analogously to previous experiences (Carpinteri et al. 2007, Carpinteri et al. 2008) of the authors, it has been recognized a link between the AE locations and the damage zones computed by the numerical model. In addition, it has been found a correlation between the AE counting and the evolution of the imposed displacement (Figure 11), of the same kind as the one shown in Figure 16, concerning a full scale masonry vault.

ACKNOWLEDGMENTS

The model bridge construction as well as the dynamic acquisition and identification were performed under the MIUR grant “Linee guida per la sorveglianza e la gestione delle strutture e infrastrutture storiche con il supporto di tecniche innovative per il monitoraggio strumentale”. The collaboration of Prof. Alessandro De Stefano and Ing. Gianluca Ruocci is gratefully acknowledged.

REFERENCES

- Carpinteri, A. & Bocca P. eds. 1991. Damage and Diagnosis of Materials and Structures. *Proc. of DDMS 91*, Politecnico di Torino, Bologna: Pitagora Editrice.
- Carpinteri, A. & Lacidogna, G. 2001. Monitoring a masonry building of the 18th century by the acoustic emission technique. *Proc. of the 7th International Conference on Structural Studies, Repairs and Maintenance of Historical Buildings* 327-337.
- Carpinteri, A., Invernizzi, S. & Lacidogna, G. 2007. Structural assessment of a XVIIth century masonry vault with AE and numerical techniques. *International Journal of Architectural Heritage* 1(2):214-226.
- Carpinteri, A., Lacidogna, G. 2006. Damage monitoring of a fan historical masonry building by the acoustic emission technique. *Materials and Structures* 39:161-167.
- Carpinteri, A., Lacidogna, G., Invernizzi, S., Manuello, A. & Binda, L. 2008. Stability of the vertical bearing structures of the Syracuse Cathedral: Experimental and numerical evaluation. *Materials and Structures* 42(7):877-888.
- Manie, J. 2009. *DIANA - Finite Element Analysis User's Manual rel. 9.3*, TNO DIANA BV Schoemakerstraat 97, 2628 VK Delft, The Netherlands.
- Ohtsu, M. 1996. The history and development of acoustic emission in concrete engineering. *Magazine of Concrete Research* 48:321-330.
- Royles, R. & Hendry, A.W. 1991. Acoustic emission monitoring of masonry arch bridges. *Proc. Inst. Civ. Engr., Part 2*, 91:299-321.